

Transfer Processes in the Flow of Gases Through Packed and Distended Beds of Spheres

J. T. L. McCONNACHIE and GEORGE THODOS

The Technological Institute, Northwestern University, Evanston, Illinois

Simultaneous mass, heat, and momentum transfer was experimentally investigated for the flow of air through packed and distended beds of spheres saturated with water. The porous spheres were approximately $\frac{5}{8}$ in. in diameter. The void fraction of the packed bed was $\epsilon = 0.416$, and the distended beds, whose spheres were positioned in a body-centered cubic arrangement, had respective void fractions of $\epsilon = 0.576$ and 0.778 . The distended beds were formed by separating the spheres and connecting them with short lengths of fine rigid wire.

Similar relationships for the packed and the distended fixed beds were obtained when the transfer factors were related to the modified Reynolds number. The relationship obtained for mass transfer in packed and distended beds was found to apply to data reported for fluidized beds of spheres.

Pressure drop measurements were made which were not exacting but which indicate that the Ergun relationship for packed beds can be used to relate the friction factor to the modified Reynolds number for both the packed and distended beds investigated.

Several past investigations have been concerned with the transfer of mass, heat, and momentum for the flow of fluids through packed and fluidized beds of particles to establish transfer coefficients for these processes (4, 6, 7, 8, 10, 11). The recent study of De Acetis and Thodos (2) showed that the relationships between heat and mass transfer factors and the modified Reynolds number $N_{Re} =$

$D_p G / \mu$ were the same for the flow of air through packed fixed beds of porous spheres and through expanded fixed beds containing randomly dispersed solid plastic spheres. Since the plastic and the porous spheres have the same volume, both types of beds were of the same void fraction. It would be of interest to determine if similar relationships are obtained for expanded fixed beds of varying void fractions in which the separated spheres are held in position. Therefore in this study the simultaneous

mass and heat transfer and pressure drop relationships for the flow of air through this type of packing were investigated.

EXPERIMENTAL EQUIPMENT AND PROCEDURE

The experimental unit used was the same as that described by De Acetis and Thodos (2) and consisted of two sections constructed with copper pipe. The lower part of the unit contained the reactor and was fixed in position, while the upper part which contained the calming section



Fig. 1. Close-up view of distended, fixed bed in a body-centered cubic arrangement ($\epsilon = 0.576$).

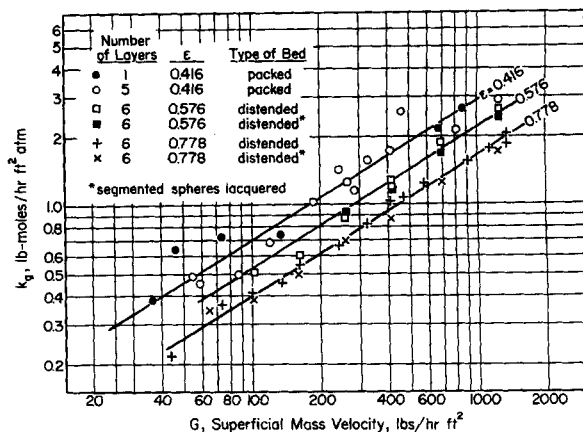


Fig. 2. Relationships between mass transfer coefficient k_g and superficial mass velocity G for packed and distended beds of varying void fractions.

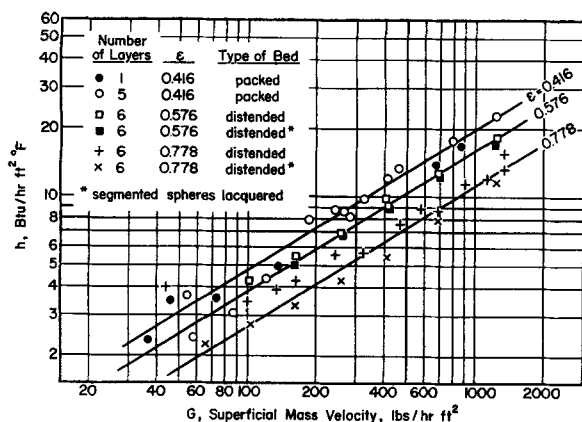


Fig. 3. Relationships between heat transfer coefficient h and superficial mass velocity G for packed and distended beds of varying void fractions.

could be disengaged to remove and weigh the reactor and determine the rate of water evaporation. The cylindrical reactor unit was initially constructed of stainless steel and later of plastic to minimize radial heat transfer. Both reactor units were 3.692 in. in diameter and 3¼ in. high. A screen was fixed at the bottom of the reactor to support the packed bed.

For these studies the beds were made of porous spheres, 0.625 in. in diameter which were capable of absorbing sufficient quantities of water to exhibit constant drying rates. Several spheres were provided with fine wire thermocouples by drilling through a major diameter and inserting the wire through the hole until the junction reached a point just below the opposite surface.

The spheres were arranged into both packed beds and distended fixed beds. The packed beds, consisting of five layers of twenty-seven spheres each, had void fractions of $\epsilon = 0.416$, and were placed in the unit above the reactor screen. The spheres containing the thermocouples were randomly distributed throughout the bed. To avoid saturated conditions at the exit of the bed for low flow rates a packed bed was prepared, which consisted of one layer of porous spheres sandwiched between four layers of solid plastic spheres which could not absorb water.

The distended fixed beds which were utilized to simulate fluidized beds were prepared by placing the spheres, some of which contained thermocouples, in a body-centered cubic arrangement and then separating them with short lengths of fine rigid wire capable of supporting this structure. The wires were permanently attached to the spheres by inserting them into holes drilled in the spheres at the proper angles and injecting epoxy resin with a hypodermic needle. In order to eliminate wall effects in the reactor which would be more pronounced for this type of arrangement each distended bed was placed in a cylindrical container of water. The contents of the container were then frozen solid with dry ice, after which the container was removed. The frozen cylindrical structure was turned on a lathe to reduce the diameter of the distended bed to the diameter of the reactor, so the bed could fit tightly in the reactor. The ice was then melted and the spheres were dried. In order to eliminate the nonspherical surfaces from participating in the mass and heat transfer processes a thin coat of epoxy resin was applied to these surfaces. The resulting distended bed was then placed in the reactor without the screen, and a number

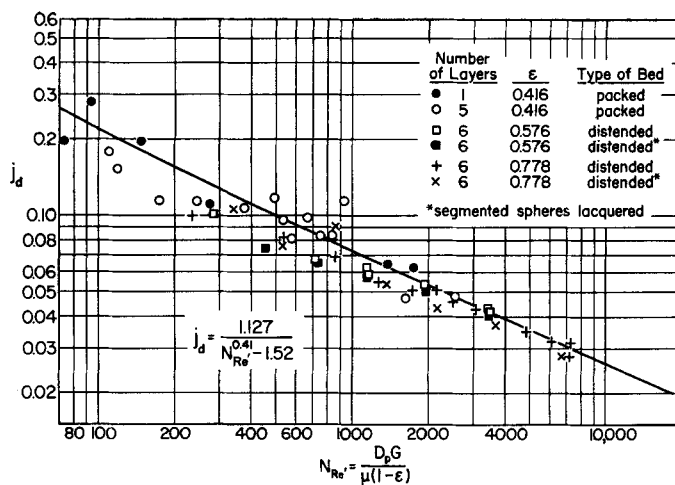


Fig. 4. Relationship between mass transfer factor j_d and modified Reynolds number $D_p G / \mu (1 - \epsilon)$ for packed and distended fixed beds of varying void fractions.

of experimental runs were conducted. In addition several runs were made in which the spherical segments adjacent to the wall surface were completely eliminated from mass and heat transfer by lacquering them. This modification did not appear to influence the results. One distended bed had a void fraction of $\epsilon = 0.576$, but the other had a void fraction of $\epsilon = 0.778$. A close up view of the distended fixed bed having a void fraction of $\epsilon = 0.576$ is given in Figure 1.

In a typical run the reactor unit with included spheres and attached thermocouples was submerged in distilled water for at least 2 hr. until the spheres were saturated. Air flow rates were measured with a rotameter. The air leaving the rotameter was forced through a small glass unit provided with thermometers and thermocouples for measuring its dry- and wet-bulb temperatures to establish the partial pressure of water vapor in the inlet air. After leaving the reactor the dry- and wet-bulb temperatures of the air were again measured to determine if the air leaving the bed were saturated. Pressure taps before and after the reactor unit were connected to an inclined manometer to determine the absolute pressures at these

TABLE 1. EXPERIMENTAL DATA AND DERIVED QUANTITIES FOR TYPICAL RUNS OF PACKED AND DISTENDED BEDS OF SPHERES

$D_p = 0.0521$ ft. (0.625 in.) (all fractional spheres participating in mass and heat transfer operation)

Run no.	Temperatures, °F.					G, lb./hr. sq. ft.	Pressure drop ΔP, lb./sq. ft.	$r \times 10^3$, lb.-moles/hr.	q , B.t.u./hr.	k_g , lb.-moles/hr. sq. ft. atm.	h , B.t.u./hr. sq. ft. °F.	j_d	j_h	f_k	$D_p G/\mu (1 - \epsilon)$
	π , mm.	t_{d_1}	t_{w_1}	t_{d_2}	t_s										
$\epsilon = 0.416$, $a = 94.7$ sq. ft./cu. ft., $aV = 1.154$ sq. ft., $L = 0.232$ ft. (2.78 in.)															
10	748.4	75.5	53.4	56.8	54.5	120.4	0.104	2.51	42.72	0.683	4.38	0.114	0.121	6.02	245
4	749.7	75.2	53.3	55.6	53.6	243.3	0.140	4.63	83.23	1.424	8.77	0.118	0.120	2.05	495
6	752.0	76.1	53.1	56.8	53.5	325.6	0.249	6.05	110.9	1.581	9.72	0.099	0.099	2.03	662
7	751.7	78.0	53.2	59.3	54.0	801.0	1.249	13.52	253.4	2.130	17.70	0.047	0.074	1.70	1,620
11	749.7	78.3	54.4	63.0	55.3	1,255	2.695	19.66	370.3	2.903	22.90	0.048	0.061	1.50	2,532
$\epsilon = 0.576$, $a = 47.1$ sq. ft./cu. ft., $aV = 0.758$ sq. ft., $L = 0.216$ sq. ft. (2.59 in.)															
47	749.1	72.3	51.3	57.8	53.9	101.7	0.005	1.82	30.22	0.510	4.27	0.101	0.140	1.69	284
45	732.1	75.7	53.0	61.9	54.7	257.1	0.021	3.87	68.13	0.880	6.97	0.068	0.090	1.03	718
44	745.0	75.7	53.7	63.2	54.8	410.6	0.067	5.01	90.40	1.196	8.70	0.059	0.071	1.33	1,146
49	747.2	71.9	50.6	61.3	50.8	692.0	0.150	7.56	139.2	1.845	12.04	0.054	0.058	1.06	1,933
48	749.2	72.7	50.8	63.6	51.2	1,254	0.430	11.44	213.4	2.567	17.12	0.042	0.046	0.94	3,500
$\epsilon = 0.778$, $a = 22.7$ sq. ft./cu. ft., $aV = 0.470$ sq. ft., $L = 0.278$ sq. ft. (3.34 in.)															
33	746.7	80.5	58.8	65.7	62.9	44.0	—	0.83	11.61	0.218	4.00	0.099	0.268	—	235
28	745.9	84.3	58.4	76.9	59.8	322.8	—	3.24	53.14	0.821	5.61	0.051	0.058	—	1,721
27	742.2	83.9	59.0	76.8	59.5	578.3	0.010	4.88	84.52	1.242	8.87	0.043	0.051	0.36	3,086
24	742.8	83.4	57.0	75.3	58.4	907.2	0.067	6.22	110.2	1.549	11.53	0.035	0.042	1.02	4,838
34	747.6	75.0	54.2	70.9	54.6	1,366	0.192	6.15	110.6	2.077	13.14	0.032	0.032	1.31	7,285

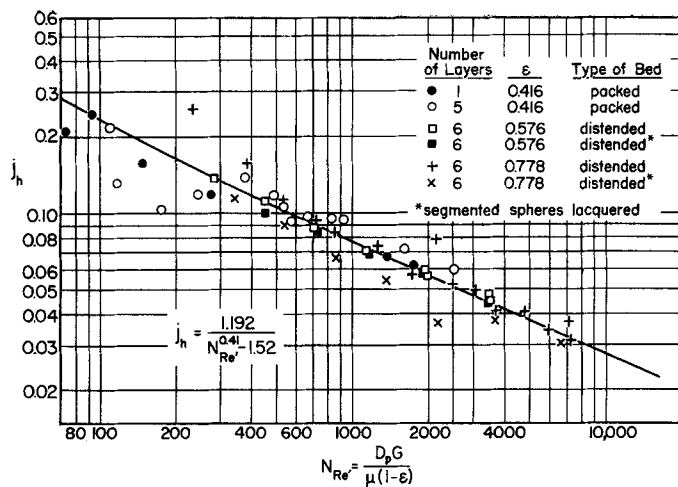


Fig. 5. Relationship between heat transfer factor j_h and modified Reynolds number $D_p G / \mu (1 - \epsilon)$ for packed and distended fixed beds of varying void fractions.

points. In order to facilitate the removal of the reactor cartridge the several thermocouple junctions were connected to a multi-point contact connector. The removal, weighing, and repositioning of the reactor cartridge consumed approximately 30 sec. The operating interval between weighings varied from 5 to 30 min. depending on the air flow rate.

INTERPRETATION OF DATA

The experimental data obtained for both the packed and distended fixed beds were utilized to establish k_o and h , the mass and heat transfer coefficients in the equations

$$r = k_o a V (\Delta p)_m \quad (1)$$

and

$$q = h a V (\Delta t)_m \quad (2)$$

Since the temperature on the surface of the spheres was measured directly with thermocouples, the resulting values of k_o and h are independent of each other, in contrast to the values which resulted from the study of Gamson, Thodos, and Hougen (4), who assumed that the surface temperature was the same as the wet-bulb temperature of the inlet air.

The data and derived quantities of a limited number of runs are presented in Table 1. A complete listing of the data and derived quantities for the fifty-seven runs of this study can be found elsewhere (9). In Figure 2 the derived quantity k_o is related to the superficial mass velocity G on log-log coordinates to produce separate linear relationships for each void fraction. Similarly in Figure 3 the heat transfer coefficient h is related to G to produce a linear relationship for each void fraction. In the calculation of the heat transfer coefficients the effect of the heat added to the spheres from the walls through radiation was calculated by assuming blackbody conditions and

by assuming that the source temperature was the same as the average dry-bulb temperature of the air flowing through the bed. The sink temperature was the temperature prevailing on the surfaces of the spheres. Since the non-spherical segments adjacent to the walls were coated with epoxy resin, the heat effect of conduction from the walls to the spheres was neglected. A separate investigation is required to measure precisely the effects of conduction and radiation in experiments of this type. The calculated radiation effect was subtracted from the total heat absorbed by the spheres (calculated from the rate of evaporation) to produce the value of q used with Equation (2). In a typical run (Run 4), the total heat absorbed was calculated to be 88.49 B.t.u./hr. and the radiation effect 5.26 B.t.u./hr. to produce a net heat transfer due to convection of 83.23 B.t.u./hr.

The mass and heat transfer coefficients were utilized to establish the

mass and heat transfer factors proposed by Chilton and Colburn (1):

$$j_d = \frac{k_o p_{sf}}{G/M} \left(\frac{\mu}{\rho D_o} \right)^{2/3} \quad (3)$$

$$j_h = \frac{h}{c_p G} \left(\frac{c_p \mu}{k} \right)^{2/3} \quad (4)$$

Mass transfer data for the fifty-seven runs of this study were analyzed to produce the corresponding mass transfer factors. In their calculation the Schmidt group for average film conditions was approximately 0.607. In Figure 4 the resulting j_d factors are related to the modified Reynolds number $D_p G / \mu (1 - \epsilon)$ and produce a single relationship for both fixed and distended beds in the high Reynolds region. In the low Reynolds region some scattering is encountered which may be attributed to significant back-mixing effects. The best analytic relation for the entire region may be expressed as follows:

$$j_d = \frac{1.127}{N_{Re'}^{0.41} - 1.52} \quad (5)$$

Heat transfer factors j_h were calculated following an analogous approach. In these calculations the Prandtl group at average film conditions was 0.719. The resulting j_h factors were plotted against the modified Reynolds number $D_p G / \mu (1 - \epsilon)$ on log-log coordinates to produce the relationship of Figure 5 for both packed and distended fixed beds. Again some scattering was found to exist in the low Reynolds region. This relationship may be expressed analytically as

$$j_h = \frac{1.192}{N_{Re'}^{0.41} - 1.52} \quad (6)$$

The j_d and j_h factors resulting from this study are compared with those of

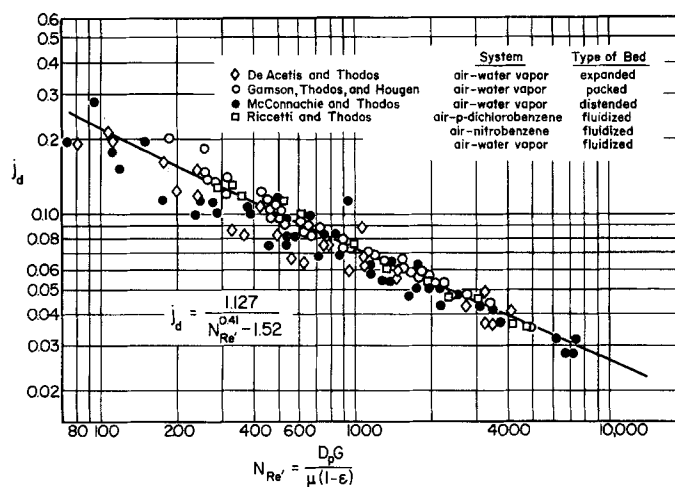


Fig. 6. Comparison of mass transfer factors resulting from this study with the data of other investigators.

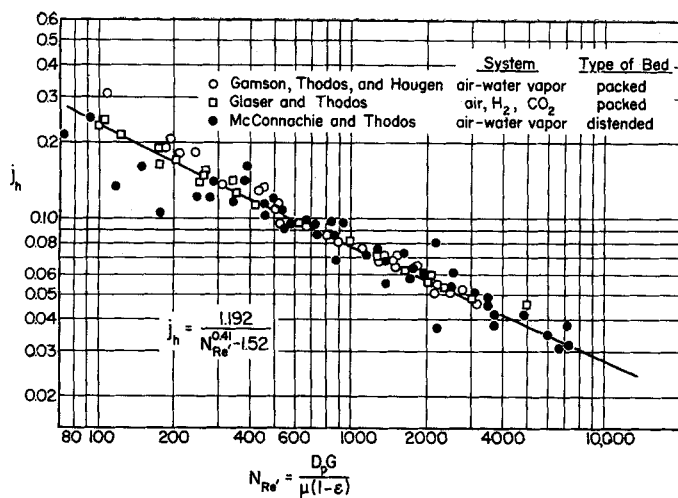


Fig. 7. Comparison of heat transfer factors resulting from this study with the data of other investigators.

other investigators in Figures 6 and 7, respectively. Figure 6 indicates that the mass transfer factors of this investigation are consistent with those of Gamson, Thodos, and Hougen (4) for packed beds, De Acetis and Thodos (2) for expanded beds, and Riccetti and Thodos (8) for fluidized beds. It may be seen from Figure 7 that the heat transfer factors resulting from this study are consistent with those reported in the study of Glaser and Thodos (5), in which metallic spheres were heated electrically, and the surface temperature of the spheres was measured directly with thermocouples. The heat transfer factors of this study are also in agreement with those of Gamson, Thodos, and Hougen (4), who assumed that the surface temperature was the same as the wet-bulb temperature of the inlet air and did not correct for conduction and radia-

tion effects. Thus this latter agreement may be somewhat fortuitous in that several effects are counterbalanced. However the j_h factors reported by De Acetis and Thodos (2), who did not correct for radiation and conduction effects, were found to be inconsistent with the others and consequently were eliminated from this comparison. The ratio of j_h/j_a resulting from Equations (5) and (6) is 1.058 as compared with the value of 1.51 reported by De Acetis and Thodos (2) and 1.08 reported by Gamson, Thodos, and Hougen (4) for packed beds.

PRESSURE DROP MEASUREMENTS

In each experimental run pressure drop measurements were conducted with a 1-in. inclined manometer (special grade = 0.827). These mea-

surements were not exacting but were made to establish pressure conditions at the inlet and outlet of the reactor and are presented in Table 1. The pressure drops for the distended bed having the highest void fraction ($\epsilon = 0.778$) were small and difficult to measure accurately. Their maximum value was 0.037 in. of water.

Ergun (3) has proposed the following relationship for pressure drops through packed beds of spheres

$$g_c \frac{\Delta p D_p}{\rho u^2 L} \frac{\epsilon^3}{1 - \epsilon} = \frac{150}{D_p G / \mu (1 - \epsilon)} + 1.75 \quad (7)$$

where the quantity $g_c \frac{\Delta p D_p}{\rho u^2 L} \frac{\epsilon^3}{1 - \epsilon}$

represents the friction factor f_k . For the packed and distended beds of this study values of the friction factor were calculated with the experimental pressure drop measurements and were plotted vs. the corresponding modified Reynolds number $D_p G / \mu (1 - \epsilon)$, as shown in Figure 8. Although considerable scattering is evidenced, these rough pressure drop measurements indicate that the Ergun relationship of Equation (7) applies to both packed and distended fixed beds.

CONCLUSIONS

Figure 6 indicates that the mass transfer factors for distended fixed beds which result from this study are consistent with the mass transfer factor obtained by other investigators for packed and fluidized beds. Therefore the motion of the particles in a fluidized bed does not appear to have a significant effect on the mass transfer process. Figure 7 indicates that the heat transfer factors resulting from this study are consistent with those of Glaser and Thodos (5) for packed beds, suggesting that the relationship of Figure 7 could also be applied to fluidized beds. Also this study indicates that there is essentially no difference between the j_h and j_a relationships for expanded fixed beds formed by randomly dispersed solid spheres and those formed by holding the separated spheres in position.

NOTATION

- a = effective surface area of spheres per unit volume, sq. ft./cu. ft.
- c_p = heat capacity at constant pressure, B.t.u./lb. °F.
- D_p = sphere diameter, ft.

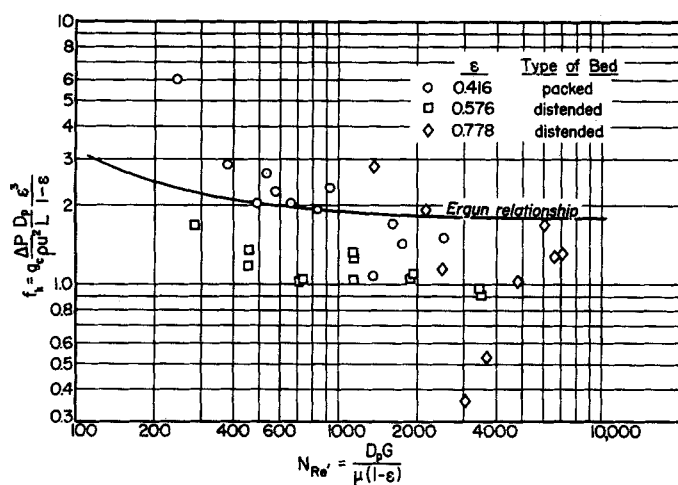


Fig. 8. Relationship between friction factor f_k and modified Reynolds number $D_p G / \mu (1 - \epsilon)$ for packed and distended fixed beds of varying void fractions.

D_v	= diffusivity of transferable component, sq. ft./hr.	N_{Re}	= modified Reynolds number, $D_p G/\mu$
f_k	= friction factor for packed beds, $g_o \frac{\Delta P}{\rho u^2} \frac{D_p}{L} \frac{\epsilon^3}{1-\epsilon}$	$N_{Re'}$	= modified Reynolds number, $D_p G/\mu(1-\epsilon)$
g_o	= conversion factor, 32.17 lb.m/ft./lb.r. sec. ²	P	= pressure, atm.
G	= superficial mass velocity, lb.m/hr. sq. ft.	$(\Delta p)_m$	= log-mean partial pressure difference of transferable component, atm.
h	= heat transfer coefficient, B.t.u./hr. sq. ft. °F.	p_{vf}	= partial pressure of nontransferable component, atm.
i_d	= mass transfer factor, $\frac{k_p p_{vf}}{G/M}$	q	= rate of convective heat transfer, B.t.u./hr.
	$\left(\frac{\mu}{\rho D_v}\right)^{2/3}$	r	= rate of mass transfer, lb.-moles/hr.
i_h	= heat transfer factor, $\frac{h}{c_p G}$	t	= temperature, °F.
	$\left(\frac{C_p \mu}{k}\right)^{1/3}$	$(\Delta t)_m$	= log-mean temperature difference across gas film, °F.
k	= thermal conductivity, B.t.u./hr. ft. °F.	t_{d_1}	= temperature of inlet air, °F.
k_g	= mass transfer coefficient, lb.-moles/hr. sq. ft. atm.	t_{d_2}	= temperature of outlet air, °F.
L	= bed height, ft.	t_s	= surface temperature of spheres, °F.
M	= molecular weight	t_w	= wet-bulb temperature, °F.
		u	= superficial velocity, ft./sec.
		V	= volume of reactor, cu. ft.
		ϵ	= void fraction of bed
		μ	= viscosity, lb.m/sec. ft.
		ρ	= absolute density, lb.m/cu. ft.

LITERATURE CITED

1. Chilton, T. H., and A. P. Colburn, *Ind. Eng. Chem.*, **27**, 255 (1935).
2. De Acetis, James, and George Thodos, *ibid.*, **52**, 1003 (1960).
3. Ergun, Sabri, *Chem. Eng. Progr.*, **48**, 89 (1952).
4. Gamson, B. W., George Thodos, and O. A. Hougen, *Trans. Am. Inst. Chem. Engrs.*, **39**, 1 (1943).
5. Glaser, M. B., and George Thodos, *A.I.Ch.E. Journal*, **4**, 63 (1958).
6. Hobson, Merk, and George Thodos, *Chem. Eng. Progr.*, **45**, 517 (1949).
7. Hurt, D. M., *Ind. Eng. Chem.*, **35**, 522 (1943).
8. Riccetti, Richard E., and George Thodos, *A.I.Ch.E. Journal*, **7**, 442 (1961).
9. McConnachie, J. T. L., M.S. thesis, Northwestern Univ., Evanston, Illinois (1961).
10. McCune, L. K., and R. H. Wilhelm, *Ind. Eng. Chem.*, **41**, 1124 (1949).
11. Wilke, C. R., and O. A. Hougen, *Trans. Am. Inst. Chem. Engrs.*, **41**, 445 (1945).

Manuscript received June 1, 1961; revision received December 18, 1961; paper accepted December 20, 1961.

Enthalpy of Nonideal Solutions: *n*-Butanol-Benzene

PAUL T. SHANNON, DAVID B. GUSTAFSON, and PATRICK S. O'NEILL

Purdue University, Lafayette, Indiana

This investigation continues the study of the thermodynamic properties of paraffinic alcohols, which exhibit considerable hydrogen bonding, and their nonideal mixtures with nonpolar compounds. This program was started by McCracken and Smith (8, 9), who studied the methanol-benzene system, and continued by Storvick (14, 15), who investigated the systems of ethanol-benzene and *n*-pentane-benzene.

In this investigation enthalpies of *n*-butanol and binary mixtures of 75, 50, and 25 mole % *n*-butanol in benzene were measured in an adiabatic flow calorimeter at temperatures from 250° to 550°F. and pressures from 20 to 1,000 lb./sq. in. abs. This range of temperature and pressure covered the vapor, liquid, and two-phase regions for all the systems studied. For the

mixtures the heat of mixing data supplied by R. V. Mrazek (10) were used to refer all mixture enthalpies relative to the pure liquid components. All enthalpy values reported (British thermal units per pound of solution) are based on the reference state of the pure liquid components at 77°F. and their vapor pressure in which state the enthalpy was arbitrarily taken to be zero.

PREVIOUS WORK

Benzene

McCracken (8) determined the pressure-enthalpy diagram for benzene over a pressure range of 0 to 1,000 lb./sq. in. abs. and a temperature range of 250° to 500°F. All thermodynamic properties of benzene used in this work for calculations or comparisons were obtained from McCracken's work as preliminary runs made with

benzene in the calorimeter were found to agree within experimental error with McCracken's results.

n-Butanol

Shemilt, Esplen, and Mann (13) who measured P-V-T properties of pure *n*-butanol from 386° to 580°F. over a pressure range of 100 to 1,000 lb./sq. in. abs. give an excellent summary of the thermodynamic data available in the literature for pure normal butanol. In constructing the pressure-enthalpy diagram for pure normal butanol the vapor pressure and latent heat data of Shemilt et al. were used as their calculated latent heats agreed with the experimental values measured at 450° and 500°F. in this work.

In addition to the data reported from the literature by Shemilt, Ingle and Cady (4), while determining molecular weights of butanol vapor near the boiling point, found that as

D. B. Gustafson is with the Monsanto Chemical Company, Springfield, Massachusetts. P. S. O'Neill is with Linde Laboratories, Tonawanda, New York.